DOI 10.1007/s11182-018-1313-x

Russian Physics Journal, Vol. 60, No. 11, March, 2018 (Russian Original No. 11, November, 2017)

THERMAL STABILITY OF MICROSTRUCTURE AND MICROHARDNESS OF HETEROPHASE BCC-ALLOYS AFTER TORSIONAL DEFORMATION ON BRIDGMAN ANVILS

I. A. Ditenberg[1,2] and A. N. Tyumentsev[1,2]

UDC 538.911; 548.4; 669.17; 620.186.8

The results of investigations of thermal stability of microstructure and microhardness of alloys of the V–4Ti–4Cr *and* Mo–47Re *systems, subjected to torsional deformation by high quasi-hydrostatic pressure at room temperature, are reported. It is shown that submicrocrystalline and nanocrystalline states, and the respective high values of microhardness, persist up to the upper bound (~0.4 T_{melt}) of the temperature interval of their recovery and polygonization in a single-phase state. The main factors ensuring thermal stability of highly-defective states in heterophase alloys are discussed.*

Keywords: BCC-alloys based on vanadium and Mo–Re, large plastic deformations, high-pressure torsion, microhardness, transmission and scanning electron microscopy, submicrocrystalline and nanocrystalline states, thermal stability.

INTRODUCTION

An investigation of the formation of submicrocrystalline (SMC) and nanocrystalline (NC) states in metal materials of different classes using the methods of large plastic deformations (LPDs) is among the most important issues of the physical materials science. At present there are only a limited number of studies dealing with the features of LPDs in BCC-metals and alloys. It is well known [1–4] that in high-strength brittle Group VI A metals of the Mendeleev's periodic table (Cr, Mo, W) high values of large plastic deformation can be commonly achieved at elevated temperatures only. In more ductile metals and alloys based on V, Nb, Ta, and Mo–Re high degrees of strain are achievable without increasing the temperature [5–9], and occasionally even at the liquid nitrogen temperature [10].

Among the critical issues for forming SMC and NC states is determination of their thermal stability and its effect on the level of mechanical properties. A generalized review of the literature data made in [1] indicates that many of the pure FCC- and BCC-metals in the course of transition into these states are characterized by a significant decrease in the recrystallization temperature, which eventually affects their properties. Despite the fact that the alloys based on refractory BCC-metals with an effective dispersion hardening or/and solid-solution hardening have been long used as structural materials for extreme service conditions, today there are too few works dealing with thermal stability of highly defective nanostructural states formed in them by the LPD methods.

In this work we perform an investigation of the thermal stability of microstructure and microhardness of a number of BCC-alloys based on V and Mo–47Re after their plastic deformation using high-pressure torsion at room temperature.

[1]Institute of Strength Physics and Materials Science of the Siberian Branch of the Russian Academy of Sciences, Tomsk, Russia, e-mail: ditenberg_i@mail.ru; [2]National Research Tomsk State University, Tomsk, Russia, e-mail: tyuments@phys.tsu.ru. Translated from Izvestiya Vysshikh Uchebnykh Zavedenii, Fizika, No. 11, pp. 128–133, November, 2017. Original article submitted July 5, 2017.

TABLE 1. Values of Shear (γ) and True Logarithmic Strain (e) Versus R and N

R, mm	e, γ	$N = 1$	$N = 5$
0.5	γ	20.9	104.7
	e	3.0	4.7
1.5	γ	62.8	314
	e	4.1	5.8
3.5	γ	146.5	732.7
	e	5.0	6.6

MATERIALS AND EXPERIMENTAL PROCEDURE

The following alloys are used in this study: a vanadium alloy of the V–4Ti–4Cr system (V–4.36Cr–4.21Ti–0.013C– 0.011N–0.02O, wt.%) and the Mo–47Re-base alloys (Mo–47Re and Mo–47Re–0.4Zr–C, N, O, wt.%). To begin with, it should be noted that the presence of a large content of interstitial impurities transforms these alloys into the class of heterophase materials [11, 12]. The heterophase structure of the V–4Ti–4Cr alloy represents high-carbon particles of vanadium oxycarbonitride, precipitated during cooling, doped with titanium and chromium [11]. The availability of a large content of carbon in the Mo–47Re–Zr alloy during heat treatments results in the formation of zirconium carbide (ZrC) characterized by non-uniform spatial distribution by volume fraction and fine size [12].

Before deformation, the ingots of the alloys under study were subjected to 1-h vacuum annealing at the temperatures 1400 and 1600°C, respectively. The specimens shaped as discs, whose thickness was 0.2 mm (0.15 mm after deformation) and diameter – 8 mm, were deformed by torsion at high quasi-hydrostatic pressure (~7 GPa) at room temperature. The number (N) of revolutions of the anvil was 1 and 5. Table 1 presents the estimated values of shear- ($\gamma = 2\pi NR/h$) and true logarithmic ($e = \ln\gamma$) strains with respect to the distance from the center of the disc (R) and the number of rotations (N).

After deformation the specimens of the V–4Ti–4Cr and Mo–47Re alloys were annealed in vacuum for one hour at the temperatures 600 and 800°C and 800, 1400 and 1600°C, respectively.

Their structural investigations were performed in a Philips CM-30 STEM-TWIN (300 kV) transmission electron microscope. In order to form thin foils in the cross section normal to the plane of the anvil, a copper layer ≈3 mm in thickness was electrolytically deposited on the specimen measuring (5–6)×2×0.2 mm. Flat workpieces in the specified cross section were cut using an electrospark discharge machine and mechanically ground to a thickness of about 100 μm. Further thinning was carried out by argon ions at the accelerating voltage 5 kV.

The EBSD patterns were obtained and analyzed using an FEI Quanta 200 3D scanning electron-ion microscope combined with a Pegasus add-on device at the accelerating voltage 30 kV in the hexagonal-packed arrangement of points. The Kikuchi patterns, formed by the backscattered electrons, were automatically indexed by the TSL OIM data collection system and analyzed by the respective TSL OIM analytical software program.

The microhardness (H_μ) values were determined from the Vickers indentation using a Neophot 21 metallographic microscope at the loads 0.5 and 1 N and exposure 15 s. The hardness measurements were performed in the cross-sections perpendicular to the anvil plane.

The features characterizing highly defective states were investigated using the dark-field analysis of discrete and continuous misorientations [13, 14].

RESULTS AND DISCUSSION

According to [7, 8, 14], after high-pressure torsion of the V–4Ti–4Cr and Mo–47Re alloys submicrocrystalline structure with high grain-size anisotropy is formed in them. It is clear from the bright-field images (Fig. 1) that at $N = 1$ ($e \approx 3$) the grains are elongated in the direction parallel to the anvil plane (AP). In the V–4Ti–4Cr alloy, the sizes of

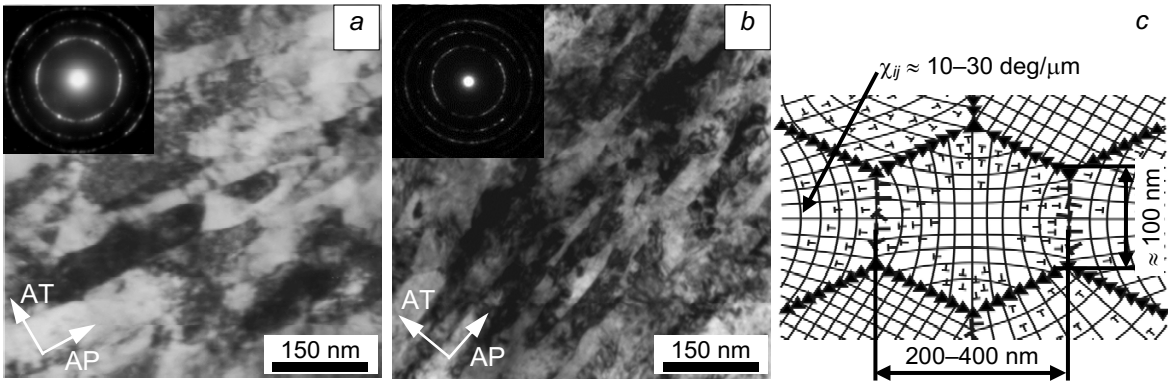

Fig. 1. Microstructure of the V–4Ti–4Cr (*a*) [8, 14] and Mo–47Re (*b*) [7] alloy specimens after deformation by high-pressure torsion ($N = 1$, $e \approx 3$). The cross section is perpendicular to the anvil plane. The scheme of a structural state with high continual density of defects (dislocations and disclinations) in the bulk and at nanocrystal boundaries [8] (*c*).

grains with high-angle boundaries along the axis of torsion (AT) fall within the interval from 50 to 200 nm (Fig. 1*a*). In the directions lying in the anvil plane, the grain size is a few times larger and is found to be within $d \approx 250$–400 nm.

The Mo–47Re alloys are characterized by the formation of inhomogeneous stripe-like structure [7]. There are both separate areas with submicron-sized grains (100–400 nm) and regions with more fragmented structure in the form of nanoscale bands whose width is about 50–70 nm (Fig. 1*b*). The electron diffraction pattern contains a high density of the diffraction maxima frequently smeared in the azimuthal direction.

It was found earlier that the maximum values of the crystal lattice curvature (χ_{ij}) in the submicrocrystals of the alloys under study are as large as a few tens of deg/μm [7, 8, 14]. Figure 1*c* schematically shows a structural model of the states with high continual density of defects (dislocations and disclinations) in the bulk and at the boundaries of submicro-sized grains [8].

As the degree of deformation is increased, there is a significant increase in the density of grains with a two-level structural state: nanofragments (measuring from 5 to 20 nm) formed inside submicro-sized grains, characterized by the dipole and multipole small-angle misorientations and elastic crystal lattice curvature of hundreds of deg/μm [7, 8]. Figure 2*a* presents a dark-field electron-microscopy image of this structural state in the Mo–Re steel subjected to deformation at $e \approx 4.7$. The defect substructure scheme with the dipole character of misorientations is given in Fig. 2*b* [8, 9, 13].

In accordance with [7, 9, 15], an increase in the density of the two-level structural states with increasing plastic deformation is followed by a considerable increase in microhardness. The highest values of H_μ in the alloys under study are observed at the maximum densities of the two-level structural states after deformation for the number of revolution $N = 5$ (TABLE 2).

In the V–4Ti–4Cr alloy, the highly defective nanostructural state and respective microhardness values persist up to the temperature 600°C (0.4 T_{melt}). It is clear from Table 2 that after deformation at $N = 5$ followed by annealing at the temperature 600°C, despite a partial relaxation (from 4.81 to 3.57 GPa), the microhardness is even slightly higher compared to the state immediately after deformation at $N = 1$ (3.44 GPa). We believe that at this temperature there is relaxation of most-highly defective states, characterized by the maximal crystal lattice curvature values up to hundreds of deg/μm.

Both microstructure and microhardness of the Mo–47Re alloys (Table 2), having high melting temperature (2500°C), are found to be stable up to the temperature 800°C (~0.4 T_{melt}). Shown in Fig. 3 are the bright-field images of microstructure of the Mo–47Re alloy after 1 (*a*) and 5 (*b*) revolutions of the anvils and subsequent annealing at 800°C. Clearly, the structural states are similar – in both cases there are microbands elongated in the direction parallel to the anvil plane. The widths of these bands vary from a few tens to hundreds of nanometers (Fig. 3*c*). Along with that, there are areas whose structural state suggests partial relaxation of the internal highly defective substructure without

TABLE 2. Average Values of Microhardness of the V–4Ti–4Cr and Mo–Re Alloys after Deformation by High-Pressure Torsion and Subsequent Anneals

Alloy	$N = 1$			$N = 5$			
	Initial [7, 15]	600°C	800°C	Initial [7, 15]	600°C	800°C	1400°C
V–4Ti–4Cr	3.44	3.27	1.87	4.81	3.57	1.97	1.5
Mo – 47% Re	10.82	–	10.48	12.87	–	12.2	4.04
Mo – 47% Re – 0.4% Zr	10.26	–	8.75	12.04	–	–	–

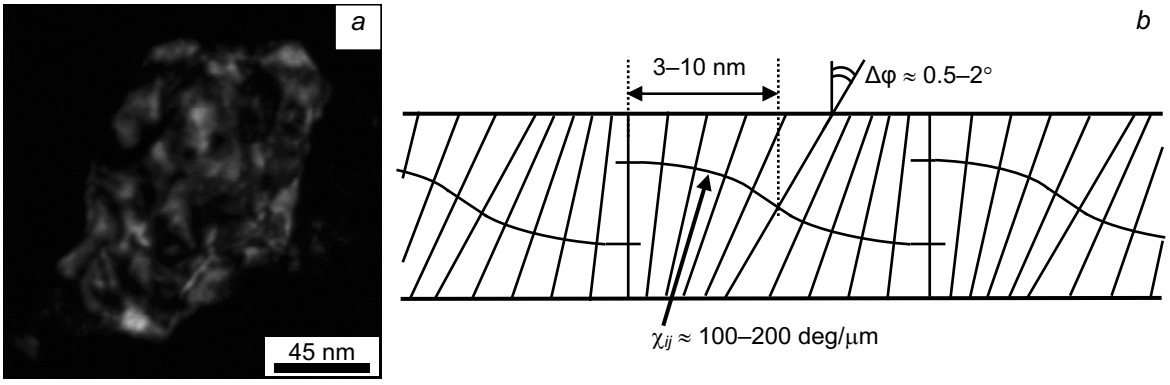

Fig. 2. Structural state of a two-level type: dark-field STEM image of the defect substructure in the Mo–Re submicrocrystalline alloy after its deformation ($e \approx 4.7$) by high-pressure torsion (*a*). The cross section is perpendicular to the anvil plane. Defect substructure scheme with dipole misorientations [8, 9, 13] (*b*).

an essential change in the grain size; there are also some bands nearly free from dislocations (Fig. 3*a*, *b*). The grain boundaries of the large-angle type are less curved in contrast to the structure immediately after deformation (Fig. 1*b*). The crystal lattice curvature is considerably lower, and its maximal values in the relaxed SMC-grains do not exceed a few deg/μm. The diffraction maxima in the microdiffraction patterns obtained from these areas, which form quasi-ring configurations, are less smeared in the azimuthal direction. An essential distinction in the microstructure of the specimens subjected to large deformations (at $N = 5$, Table 1) is a higher density of the grains with two-level states (Fig. 3*c*), which is retained after annealing.

Considerable changes in microstructure and microhardness of the V–4Ti–4Cr alloy are observed after annealing at 800°C (0.5 T_{melt}). Firstly, the grain shape undergoes considerable changes; instead of the stripe-like structure typical for the anisotropic SMC-state after high-pressure torsion (Fig. 1*a*) the grains acquire more equiaxial shape and their dimensions increase up to 0.5–2 μm (Fig. 4*a*). The starting recrystallization processes transform the microstructure into a fine-crystalline structural state without any signs of the preceding anisotropy. Secondly, the grain boundaries become more equiaxial, which is suggested by the stripe contrast (Fig. 4*b*). Thirdly, inside the grains there are no substructures with high dislocation density, nor any those with high values of the crystal lattice curvature. In addition to the above, even in the bright-field images (Fig. 4*a*, *b*) there is pepper-and-salt contrast suggesting the presence of high density of fine-sized (a few nanometers) second-phase particles typical for the dispersion-hardened states. Earlier, we observed a similar contrast pattern in the V–4Ti–4Cr alloy after thermomechanical treatment (TMT) and stabilizing annealing at $T = 1000$°C [14].

The transformation of microstructure after annealing at the temperature 800°C is accompanied by a decrease in microhardness of the V–4Ti–4Cr alloy specimens deformed at $N = 1$ up to 1.87 GPa, and at $N = 5$ – up to 1.97 GPa

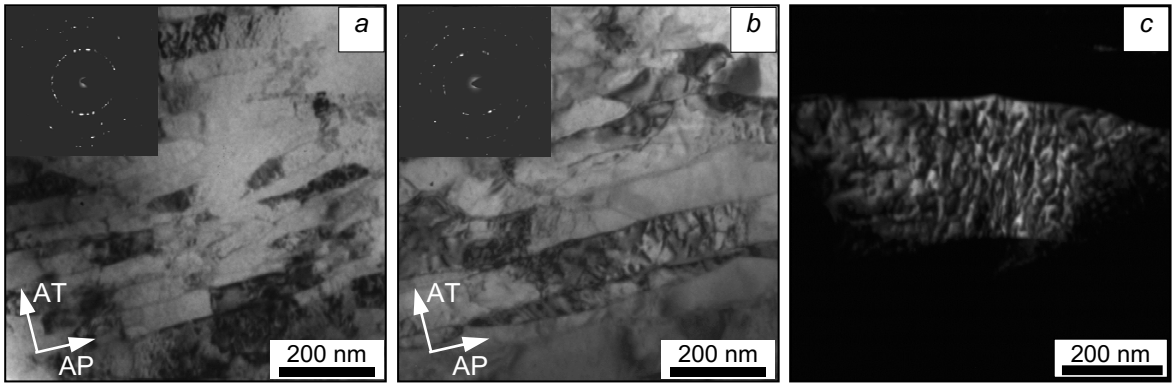

Fig. 3. Microstructure of the Mo–47Re alloy after deformation by high-pressure torsion and subsequent annealing at $T = 800$°C, $N = 1$ (*a*), $N = 5$ (*b*), a sample dark-field image of a two-level state ($N = 5$) (*c*). The cross section is perpendicular to the anvil plane.

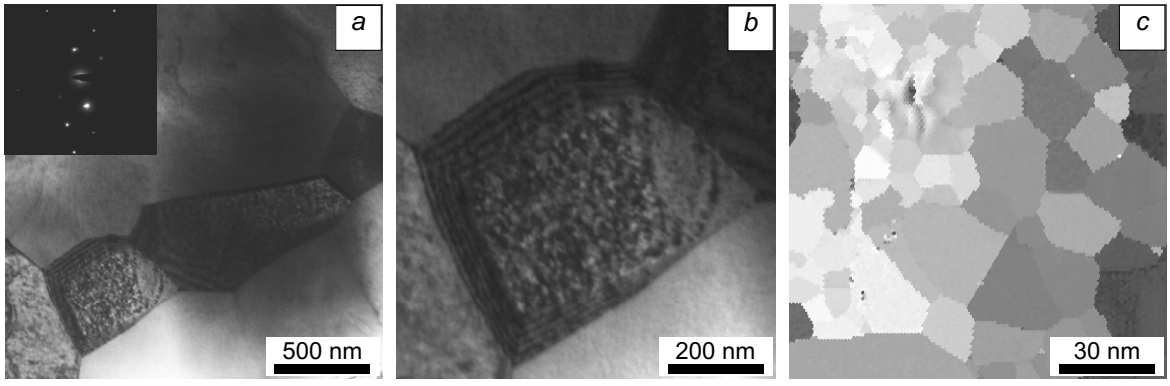

Fig. 4. Recrystallization data: TEM bright-field images of microstructure of the V–4Ti–4Cr alloy after 1-hour annealing at $T = 800$°C (*a*, *b*), SEM mapping of the grain structure angular orientation of the Mo–47Re alloy after annealing at $T = 1400$°C (EBSD) (*c*). The cross section is perpendicular to the anvil plane.

(Table 2). It should be noted that microhardness of this alloy in the coarse-grained state after 1-hour annealing at $T =$ 1400°C does not exceed 1.5 GPa (Table 2).

High spatial inhomogeneity of the elemental composition and nonuniform distribution of the second-phase particles frequently give rise to strongly inhomogeneous grain and defect structure both after LPDs and after annealing at the temperatures higher than that of recrystallization (>0.4 T_{melt}). As it is shown by the example of the Mo–47Re alloy (Fig. 4*c*) after 1-hour annealing at $T = 1400$°C (0.6 T_{melt}), the map of angular grain-structure orientation contains some regions with fine-crystalline structure (3–5 μm), areas with 10–25-μm grains and individual coarse grains measuring up to a few tens of micrometers. Thus, the structural state of the Mo–47Re alloy presented in this work is a peculiar kind of a structural composite with a complex character of spatial distribution of its structural elements (grains of different fractions). The microhardness of such a state is characterized by a considerable scatter of values, but its average values considerably decrease, reaching 4.04 GPa, due to the determinative contribution from large grains. After annealing at $T =$ 1600°C (0.675 T_{melt}), the microstructure of the Mo–47Re alloy is presented by large grains only, and the microhardness decreases to 3.03. GPa, which corresponds to the values prior to high-pressure deformation.

The persistence of the highly defective nanostructural state in the V–4Ti–4Cr alloy at the temperature of polygonization of single-phase metallic materials (~0.4 T_{melt}) results, in our opinion, from dispersion hardening by particles of the non-metallic (oxycarbonitride) phase. An increased volume content of this phase, being a consequence of the heterophase structure nanostructuring [16], is initiated by the formation of highly defective structural states. On the one hand, the latter is due to the increased solubility of the initial coarse-grained (a few tens of nanometers) precipitates in the structural states with high density of defects; on the other hand – with activation of the diffuse flows of the doping elements under the conditions of the high nonequilibrium concentration of points defects and high local stress gradients generated in the course of plastic deformation. In an earlier work [16], this approach allowed us, using the method of multiple all-round pressing, to form fine-crystalline structural state (grain size within 3–5 μm) in an alloy of the V–4Ti–4Cr system, which is stable at T = 1000°C. Thus the thermal stability of highly defective nanostructural states is to a large extent determined by that of the nanoparticles of the second phase.

CONCLUSIONS

It has been demonstrated in this study that thermal stability of highly defective nanostrtuctural states in the alloys of the V–4Ti–4Cr and Mo–47Re systems is characterized by the upper bound (~0.4 T_{melt}) of the temperature interval of manifestation of strain (substructure) hardening of many high-melting metals and alloys. Using the V–4Ti–4Cr alloy as an example, it has been shown that the achieved level of thermal stability of nanostructural state of heterophase alloys results from dispersion hardening by nanosized particles of a nonmetallic (oxycarbonitride) phase.

It has been assumed that annealing near the temperature of polygonization of single-phased metallic materials (~0.4 T_{melt}) is followed by partial relaxation of the most highly defective nanostructural states characterized by the maximum values of the crystal lattice curvature up to hundreds of deg/μm. The observed decrease in microhardness values does not exceed 25%.

The complex character of spatial distribution of the elements (grains of different fractions) of the structural composite forming in the alloys under study after anneals at the temperature higher than the recrystallization temperature (>0.4 T_{melt}) results from the high spatial inhomogeneity of the elemental composition and nonuniform distribution of the second-phase particles after LPDs.

This investigation has been performed using the facilities of the Tomsk Regional Center for Shared Use of Scientific Equipment of the National Research Tomsk State University.

The work has been carried out within the framework of the Program of the fundamental scientific research of the state academies for the years 2013–2020.

REFERENCES

1. R. Z. Valiev and I. V. Aleksandrov, Nanostructured Materials Produced by Severe Plastic Deformation [in Russian], Logos, Moscow (2000).
2. Q. Wei, H. Zhang, B. E. Schuster, *et al*., Acta Mater., **54**, Iss. 15, 4079–4089 (2006).
3. V. V. Popov, G. P. Grabovetskaya, A. V. Sergeev, *et al*., Phys. Met. Metallogr., **109**, No. 5, 556–562 (2010).
4. Yu. R. Kolobov, B. Kieback, K. V. Ivanov, *et al*., Refract. Metals & Hard Mater., No. 21, 69–73 (2003).
5. E. N. Popova, V. V. Popov, E. P. Romanov, *et al*., Phys. Met. Metallogr., **101**, No. 1, 52 – 57 (2006).
6. Q. Wei, Z. L. Pan, X. L. Wu, *et al*., Acta Mater., **59**, Iss. 6, 2423–2436 (2011).
7. S. A. Vins, I. A. Ditenberg , A. N. Tyumentsev, and Korznikova, Izv. Vyssh. Uchebn. Zaved. Fiz., **52**, 12/2 (2009).
8. I. A. Ditenberg, A. N. Tyumentsev, K. V. Grinyaev, *et al*., Tech. Phys., **56**, Iss. 6, 815–820 (2011).
9. I. A. Ditenberg, A. N. Tyumentsev, and A. V. Korznikov, Russ. Phys. J., 57, No. 12, 1683–1690 (2014).

10. V. V. Popov, E. N. Popova, A. V. Stolbovskii, et al., Phys. Met. Metallogr., **113**, No. 3, 295–301 (2012).
11. A. N. Tyumentsev, A. D. Korotaev, Yu. P. Pinzhin, *et al*., J. Nucl. Mater., **329**– **333**, 429–433 (2004).
12. V. V. Monako, A. N. Tyumentsev, A. D. Korotaev, *et al*., Fiz. Met. Metalloved., **78**, No. 1, 152–161 (1994).
13. A. N. Tyumentsev, I. A. Ditenberg, A. D. Korotaev, and K. I. Denisov, Zh. Fiz. Mezomekh., **16**, No. 3, 63–79 (2013).
14. I. A. Ditenberg, A. N. Tyumentsev, A. V. Korznikov, *et al*., Phys. Met. Metallogr., **113**, No. 2, 160–169 (2012).
15. I. A. Ditenberg, S. A. Malakhova, A. N. Tyumentsev, and A. V. Korznikov, Persp. Mater., Spec. Iss. No. 12, 306–310 (2011).
16. A. N. Tyumentsev, I. A. Ditenberg, K. V. Grinyaev, *et al*., J. Nucl. Mater., **413**, 103–106 (2011).